

Liouvillian recursion method for the electronic Green's function

A. Foley^{1,*}

¹*AlgoLab Quantique, Institut Quantique, Université de Sherbrooke, Sherbrooke, QC, Canada*
(Dated: January 8, 2024)

In this paper, we present a framework for the recursion method applied within the Liouvillian formalism, enabling the computation of response functions for a wide range of quantum operators. Indeed, unlike most previous literature on the Liouvillian recursion method, this framework readily computes electronic Green's function. We demonstrate the method by showcasing its application to a temperature dependence study of a 2×2 Hubbard model. Our results show that the recursion method accurately computes response functions and provides valuable insights into quantum many-body systems. While the method has already been successfully applied to study of condensed matter, further efforts are required to develop efficient algorithms for larger and more realistic systems. Tensor network methods and other variational techniques hold promise for tackling these challenges. Overall, the recursion method offers a flexible approach for investigating strongly correlated system.

I. INTRODUCTION

The recursion method in the Liouvillian formalism has been extensively used for the computation of response functions of hermitian operator [1–5]. However, it is not the case for response function of non-hermitian operators, such as the electronic Green's function. Indeed, the typical presentation [1, 3, 5] doesn't allow for such response function.

While Mori's original derivation [2] of the approach is applicable to the general case, it is said to be rather complicated [4, 5]. The computation of electronic Green's function is routinely done using the recursion method in the Hamiltonian formalism [1, 6–8]. This has some advantages and some drawbacks: the numerical implementation is simple and efficient, but the approach is only readily applicable in the zero temperature limit. In contrast, with the Liouvillian formalism, the approach can be carried at arbitrary temperature, but the superoperator algebra is considerably harder to implement efficiently.

In its canonical use [1, 2], the recursion method computes a response function of a finite system in the form of a continued fraction and, by analysing the structure of this continued fraction, information about the infinite size limit can be inferred. This inferred data is often interesting in its own right and from it an approximation of the response function of the infinite system can be reconstructed. The reconstruction process takes the form of an extrapolation of the continued fraction explicitly computed. It can also be used in conjunction with quantum cluster methods, sometimes with the structural analysis of the continued fraction [9, 10], but more often without [6–8]. This paper focuses on the explicit computation of continued fractions, we refer the reader to the monograph by Viswanath and Muller [1] for further reading on continued fraction analysis and extrapolation.

This paper is organized as follows: we first explain and demonstrate the method; in second, we give a few examples of functions that can be computed within this formalism, we

then show its usage with a temperature dependence study of a 2×2 Hubbard model. Finally, we present our conclusions.

II. METHOD

Definitions and notation

Going forward, we work with the natural units $k_B = \hbar = 1$, operators that are not explicitly function of time are understood to be the time-dependent operator evaluated at time $t = 0$ and the fourier transform of a function $f(t)$ is $f(\omega) = \int_{-\infty}^{\infty} f(t)e^{i\omega t} dt$.

The Liouvillian recursion method can be understood quite simply in terms of Heisenberg's equation in a superoperator formalism: the Liouvillian superoperator \mathcal{L} is the commutator of some operator with the Hamiltonian operator. Heisenberg's equation, in the Liouvillian notation read as follows:

$$-i \frac{\delta}{\delta t} \mathbf{O}(t) = \mathcal{L} \mathbf{O}(t) \equiv [\mathbf{H}, \mathbf{O}(t)] \quad (1)$$

where \mathbf{O} is some operator, \mathbf{H} is the Hamiltonian and $\mathcal{L} \equiv [\mathbf{H}, \cdot]$ is the Liouvillian. We quickly observe that in terms of this superoperator, Heisenberg's equation has the same structure as Schrödinger's equation. It consequently admits the same formal solution for time evolution:

$$\mathbf{O}(t) = e^{i\mathcal{L}t} \mathbf{O} \equiv e^{i\mathbf{H}t} \mathbf{O} e^{-i\mathbf{H}t} \quad (2)$$

This superoperator expression of the operator evolution is a well-known identity [11].

With this last observation, there's only one missing ingredient to perform the computation of response function or their associated Green's function: a scalar product for operators. While its precise definition is of little importance for the relation we will demonstrate next, the precise choice of scalar product is physically motivated: it determines what sort of response function we will compute. Concrete examples of such scalar products definitions are given in subsection II A. We denote the scalar product of two operators \mathbf{B}

* Corresponding author: Alexandre.Foley@usherbrooke.ca

and \mathbf{C} as $(B|C)$, then the response function and retarded Green's function available to the recursion method are

$$A_{BC}(t) = (B|C(t)) \quad (3)$$

$$G_{BC}(t) = -i(B|C(t))\theta(t) \quad (4)$$

respectively, for any pair of operators. In eq. (4), $\theta(t)$ is the Heaviside step function. We use parentheses to denote the scalar product instead of the more conventional angled brackets to distinguish the operation clearly from the scalar product between states, because practical definition of the operator scalar product can involve that of states.

The recursion method requires that Liouvillian is hermitian with respect to the scalar product:

$$(C|\mathcal{L}B) = (\mathcal{L}C|B) \equiv (C|\mathcal{L}|B). \quad (5)$$

With that additional property, the scalar product reproduce the usual algebra of Dirac's notation with the Hamiltonian in every way. Note that this extra property (5) is readily obtained when the scalar product is the average at thermodynamic equilibrium of some operator.

Recursion method for continued fractions

Using the time evolution identity (2), we can rewrite eq. (4) as follows:

$$\begin{aligned} G_{BC}(t) &= -i(B|e^{i\mathcal{L}t}C)\theta(t) \\ G_{BC}(t) &= -i(e^{-i\mathcal{L}t}B|C)\theta(t) \\ G_{BC}(t) &= -i(B|e^{i\mathcal{L}t}|C)\theta(t) \end{aligned} \quad (6)$$

which is a consequence of eq. (5). Since it is trivially applicable to any power of the Liouvillian, it also works with any Taylor's series and consequently any function of the Liouvillian. Next, we compute the Fourier transform with respect to time and obtain

$$G_{BC}(\omega) = (B|\frac{1}{\omega + \mathcal{L}}|C) \quad (7)$$

In the particular case where $\mathbf{B} = \mathbf{C}$, the problem amounts to computing a single diagonal element of $[\omega + \mathcal{L}]^{-1}$. This computation is readily accomplished using Lanczos' algorithm [6, 7] on the Liouvillian using \mathbf{B} as the initial operator. Lanczos' algorithm is an iterative procedure that constructs an orthogonal basis in which the target linear operator is tridiagonal. When applied to minus one times the Liouvillian, the algorithm can be expressed by the following recursive relation:

$$\beta_{k+1}\mathbf{f}_{k+1} = -\mathcal{L}\mathbf{f}_k - \alpha_k\mathbf{f}_k - \beta_k\mathbf{f}_{k-1} \quad (8)$$

$$\alpha_k = -(f_k|\mathcal{L}|f_k) \quad (9)$$

$$\beta_k = -(f_k|\mathcal{L}|f_{k-1}) \quad (10)$$

$$\mathbf{f}_{-1} = 0 \quad (11)$$

$$\mathbf{f}_0 = \frac{\mathbf{B}}{\sqrt{(B|B)}} \quad (12)$$

In the basis of \mathbf{f}_k operators and after n iterations, the Liouvillian is a tridiagonal matrix:

$$T = \begin{bmatrix} \alpha_0 & \beta_1 & 0 & \dots & 0 \\ \beta_1 & \alpha_1 & \beta_2 & \ddots & \vdots \\ 0 & \beta_2 & \alpha_2 & \ddots & 0 \\ \vdots & \ddots & \ddots & \ddots & \beta_{n-1} \\ 0 & \dots & 0 & \beta_n & \alpha_n \end{bmatrix}. \quad (13)$$

Because we used $\mathbf{f}_0 = \frac{\mathbf{B}}{\sqrt{(B|B)}}$ to initialize Lanczos' algorithm, we obtain the following expression for the Green's function:

$$G_{BB}(\omega) = (B|B) \left[\frac{1}{\omega - T} \right]_{(0,0)} \quad (14)$$

it can be shown that the (0, 0) element of the inverse matrix is a Jacobi type continued fraction [7, 12]:

$$G_{BB}(\omega) = \frac{(B|B)}{\omega - \alpha_0 - \frac{\beta_1^2}{\omega - \alpha_1 - \frac{\beta_2^2}{\ddots}}} \quad (15)$$

Continued fractions can be characterized by a number of floors; the number of divisions present in continued fractions. With Jacobi continued fractions, the number of floors counts the number of poles the function has on the neighbourhood of the real line. A Green's function with a continuous spectral weight necessarily has an infinite number of floors to its continued fraction representation. Truncation of continued fractions yields rapidly converging approximations for the purpose of computing integrals of the complete continued fraction. While this method is limited to the direct computation of diagonal elements of the Green function, it doesn't prevent us from computing off-diagonal elements as well, albeit in an indirect manner. Indeed, by computing the Green's function for the operators $\mathbf{B} + \mathbf{C}$ and $\mathbf{B} - i\mathbf{C}$ as well as for \mathbf{B} and \mathbf{C} , Lanczos' algorithm yields a continued fraction for

$$\begin{aligned} G_{BC}^r(\omega) &= (B + C|\frac{1}{\omega + \mathcal{L}}|B + C) \\ &= G_{BB}(\omega) + G_{BC}(\omega) + G_{CB}(\omega) + G_{CC}(\omega). \end{aligned} \quad (16)$$

and

$$\begin{aligned} G_{BC}^i(\omega) &= (B + iC|\frac{1}{\omega + \mathcal{L}}|B + iC) \\ &= G_{BB}(\omega) + iG_{BC}(\omega) - iG_{CB}(\omega) + G_{CC}(\omega). \end{aligned} \quad (17)$$

From those, expressions for G_{CB} and G_{BC} can be isolated. We refer to this procedure as "linear combination of continued fractions" (LCCF). In the generic case, the computational cost for off-diagonal Green's function is increased fourfold relative to computing a single diagonal element,

but it yields four Green's functions, which are often all of equal interest.

To reach an exact result, Lanczos algorithm has to be run until exhaustion of the Krylov subspace generated by the repeated action of the Liouvillian on the initial operator. Note that subspace exhaustion has happened as soon as a β coefficient is zero to working precision. In the case of electrons, this means order 4^n iterations, where n is the number of single-electron orbitals. This is often neither practical nor necessary. Indeed, this reveals a lot of information within a few tens of iterations [1], even in the limit of large n .

Recursion method for orthonormal polynomials decomposition

Within this Liouvillian framework, it is also possible to compute the decomposition of a response function on a basis of orthonormal polynomials. Orthonormal polynomial decompositions of response functions rely, as the name suggest, on orthonormal polynomials [13]. The Liouvillian version of the orthonormal polynomial method as one considerable advantage over the equivalent Hamiltonian approach: because it can compute contributions to the spectral weight of both occupied and unoccupied states at once, it doesn't have to deal with the discontinuity of the Fermi-Dirac distribution in metallic systems at zero temperature. This means faster convergence of the polynomials coefficient is expected without resorting to subtle tricks [14]. Note that hermiticity of the Liouvillian is unnecessary for this method. There are many families of orthonormal polynomial and they all share a common set of properties. Consider the set of orthonormal polynomials $\{T_n(\omega)\} \forall n \in \mathbb{Z}_{\geq 0}$. They define a function space with an inner product

$$\langle f, g \rangle = \int_a^b f(\omega)g(\omega)W(\omega)d\omega \quad (18)$$

with respect to a weight function $W(\omega)$ which is real and positive for all ω in $[a, b]$ and normalized: $\int_a^b W(\omega)d\omega = 1$. The polynomials are orthonormal with respect to this inner product:

$$\langle T_n, T_m \rangle = \delta_{nm} \quad (19)$$

The polynomials in the set are related by a three-term recurrence relation:

$$b_{k+1}T_{k+1}(\omega) = (\omega - a_k)T_k(\omega) - b_kT_{k-1}(\omega) \quad (20)$$

where the coefficients a_k and b_k are determined by the set of orthonormal polynomials, $T_0(\omega) = 1$ and $T_{-1}(\omega) = 0$. The weight function can be obtained from the coefficients of the three-term recurrence relation[citation]:

$$W(\omega) = -\lim_{\epsilon \rightarrow 0^+} \frac{1}{\pi} \text{Im} \left[\frac{1}{\omega + i\epsilon - a_0 - \frac{b_1^2}{\omega + i\epsilon - a_1 - \frac{b_2^2}{\ddots}}} \right]. \quad (21)$$

A function $f(\omega)$ defined on the domain $[a, b]$ can expressed in terms of the polynomials:

$$f(\omega) = \sum_n \mu_n T_n(\omega) W(\omega) \quad (22)$$

$$= \sum_n \nu_n T_n(\omega) \quad (23)$$

$$\mu_n = \int_a^b f(\omega) T_n(\omega) d\omega = \langle \frac{f}{W}, T_n \rangle \quad (24)$$

$$\nu_n = \int_a^b f(\omega) T_n(\omega) W(\omega) d\omega = \langle f, T_n \rangle \quad (25)$$

A few examples of such polynomial functions are Tchebyshev, Legendre, l'Hermite and Laguerre polynomials. The first two are defined on a finite domain, while Laguerre's polynomials are on a semi-infinite domain and l'Hermite's are defined for all real values. Some guesswork is needed to adapt the polynomial basis to the a priori unknown bandwidth of the Green's function.

Along with the identities introduced in II, the equations introduced in this section allow us to devise an algorithm to compute the μ -moments of a response function in the frequency domain. By performing a Fourier transform on eq. (3) we obtain:

$$A_{BC}(\omega) = (B|\delta(\omega + \mathcal{L})|C) \quad (26)$$

Then substituting $f(\omega)$ by $A_{BC}(\omega)$ in eq. (24) gives us the following:

$$\begin{aligned} \mu_n &= \int_a^b (B|\delta(\omega + \mathcal{L})|C) T_n(\omega) d\omega \\ &= (B|T_n(-\mathcal{L})|C) \\ &= (B|f_n) \end{aligned} \quad (27)$$

Where we defined $f_n = T_n(-\mathcal{L})C$. Multiplying the polynomials' three-term recursion (20) by C , we obtain

$$\begin{aligned} b_{k+1}T_{k+1}(-\mathcal{L})C &= (-\mathcal{L} - a_k)T_k(-\mathcal{L})C - b_kT_{k-1}(-\mathcal{L})C \\ \implies b_{k+1}f_{k+1} &= (-\mathcal{L} - a_k)f_k - b_kf_{k-1} \end{aligned} \quad (28)$$

The set of operators f_k can be efficiently computed to finite order without explicitly evaluating the polynomials of the superoperator.

Unlike Lanczos's algorithm, independently of system size the formal solution produced by this method is an infinite serie. This isn't much of a practical issue, because the similar nature of the recursive algorithms shows that both methods explore the same Krylov subspace and extract a similar amount of information at a similar pace. Indeed, a unique N -poles approximation of the Green's function could be reconstructed from $2N$ polynomial moments [15]. In practice, truncating the polynomial introduce Gibbs's oscillation to the reconstructed spectral weight [13]. This phenomenon can be controlled using kernel smoothing methods [13] or linear prediction [14, 16]. Finally, a striking

advantage of the polynomials decomposition is that multiple response function can be computed in a single recursive procedure: the operator \mathbf{B} does not intervene in the recursive part of the algorithm. Consequently, the decomposition of any response function that share the same \mathbf{C} operator can be computed using the same set of \mathbf{f}_k operators.

This recursive procedure produces a decomposition of the spectral weight on the chosen basis, but the Green's function can also be obtained from the same coefficients. Since the Green function and the spectral weight in the frequency domain are related by the Kramers-Kronig relations [17]. A corollary of the Kramers-Kronig relation is the analytical continuation relations:

$$G_{BC}(z) = \lim_{\epsilon \rightarrow 0^+} \frac{1}{2\pi} \int_{-\infty}^{\infty} \frac{A_{BC}(\omega)}{z - \omega + i\epsilon} d\omega, \quad (29)$$

$$A_{BC}(\omega) = - \lim_{\epsilon \rightarrow 0^+} \frac{1}{2} \text{Im}[G(\omega + i\epsilon)]. \quad (30)$$

We observe in eq. (29) that the Green function is the Stieltjes transform of the spectral weight. The theory relative to the Stieltjes transform [18–20] is deeply intertwined with the theory of orthonormal polynomials. Given a μ -decomposition of $A_{BC}(\omega)$ the solution to eq. (29) takes the form [21, 22]:

$$G_{BC}(z) = \sum_n \mu_n (U_n(z) + T_n(z)S_W(z)) \quad (31)$$

where $S_W(z)$ is the Stieltjes transform of the weight function $W(\omega)$ and $U_n(z)$ are the polynomials of the second kind associated with the weight function. If the function $S_W(z)$ is not known analytically, it can be computed using a continued fraction involving the coefficients of the three-term recurrence:

$$S_W(z) = \frac{1}{z - a_0 - \frac{b_1^2}{z - a_1 - \frac{b_2^2}{\ddots}}} \quad (32)$$

The secondary polynomials are defined by the following recurrence and initial conditions:

$$b_{k+1}U_{k+1}(z) = (z - a_k)U_k(z) - b_kU_{k-1}(z) \quad (33)$$

$$U_0(z) = 0 \quad (34)$$

$$U_1(z) = \frac{-T_1(z)}{z - a_0} \quad (35)$$

The initial conditions for the U_i polynomials are fixed by the requirement that $G_{BC}(z) \simeq \frac{(B|C)}{z}$ when $|z| \gg 1$. In other words, all polynomial contributions $z^n \forall n > 0$ must cancel out at high frequency.

On the relation between continued fractions and orthonormal polynomials

One quickly notice that Lanczos' algorithm and the orthonormal polynomial method rely on basically identical

equations. In fact, Lanczos' procedure amounts to generating a special purpose polynomial basis such that $\mu_k = (B|B)\delta_{k,0}$. Indeed, the operators generated by Lanczos procedures are mutually orthonormal with respect to our chosen scalar product and $\mu_k = (B|f_k) \equiv (f_0|f_k)$. The polynomials $L_k(\omega)$ produced by Lanczos' algorithm are defined by

$$\beta_{k+1}L_{k+1}(\omega) = (\omega - \alpha_k)L_k(\omega) - \beta_kL_{k-1}(\omega) \quad (36)$$

$$L_{-1}(\omega) = 0 \quad (37)$$

$$L_0(\omega) = 1 \quad (38)$$

Those polynomials are orthonormal with respect to the spectral weight $A_{CC}(\omega) = \lim_{\epsilon \rightarrow 0^+} \text{Im}\left(\frac{-1}{\pi}G_{CC}(\omega + i\epsilon)\right)$

$$\int_{-\infty}^{\infty} L_m(\omega)L_n(\omega)A_{CC}(\omega)d\omega = \delta_{mn} \quad (39)$$

This observation provides us an alternative way of computing off-diagonal Green's function element within Lanczos' algorithm: we can compute their moments on the Lanczos-generated polynomial basis, yielding a decomposition of the off diagonal elements $A_{BC}(\omega)$ in terms of the polynomials that are orthogonal with respect to the targeted diagonal element $A_{CC}(\omega)$.

In short, with this continued fraction-polynomial hybrid procedure (CFPH), the diagonal Green's function $G_{CC}(z)$ is given by the continued fraction generated by Lanczos' algorithm and we have the coefficients $\mu_n = (B|f_n)$ for the off-diagonal Green's function elements

$$G_{BC}(z) = \sum_n \mu_n (Q_n(z) + L_n(z)G_{CC}(z)). \quad (40)$$

Where the secondary polynomials $Q_n(\omega)$ are defined by

$$\beta_{k+1}Q_{k+1}(z) = (z - \alpha_k)Q_k(z) - \beta_kQ_{k-1}(z) \quad (41)$$

$$Q_0(z) = 0 \quad (42)$$

$$Q_1(z) = \frac{-L_1(z)}{z - \alpha_0} \quad (43)$$

This computation method has a significant advantage in comparison to either method taken alone. Compared with the LCCF method for off-diagonal elements of the Green function, it is computationally cheaper. Compared with the orthonormal polynomial computation method, there is no need to rescale the polynomials to fit the a priori unknown bandwidth of the Green's function.

For a generic L site system, with no spatial nor time-reversal symmetry, the LCCF method would have to be performed L^2 times requiring L^2k action of the Liouvillian on an operator and $2L^2k$ inner products, where k is the number of iterations performed. In contrast, the CFPH method would be performed L times requiring Lk application of the Liouvillian and $(2 + L(L - 1))k$ inner products. This is only $2k$ more inner products than the orthonormal polynomial method.

A. Examples of scalar product

The precise definition of the scalar product used determines the physical content of the response function the recursive methods compute. Here we give the scalar product's definitions for a few common uses and demonstrate that it has all the properties required of inner products [23], namely positive definiteness, conjugate symmetry and linearity, along with the hermiticity of the Liouvillian. Those scalar product will all have the form

$$(B|C) = \frac{1}{\beta} \int_0^\beta d\lambda g(\lambda) \langle e^{\lambda \mathbf{H}} \mathbf{B}^\dagger e^{-\lambda \mathbf{H}} \mathbf{C} \rangle \quad (44)$$

where the angled brackets is the thermodynamic average at inverse temperature β , $g(\lambda)$ is positive on $[0, \beta]$, $g(\beta - \lambda) = g(\lambda)$ and $\frac{1}{\beta} \int_0^\beta d\lambda g(\lambda)$ is some finite constant. The

thermodynamic average is defined as

$$\langle B \rangle = \frac{\text{Tr}[e^{-\beta \mathbf{H}} B]}{\text{Tr}[e^{-\beta \mathbf{H}}]}. \quad (45)$$

Because the average in Dirac's Hilbert space is both linear and conjugate symmetric, the linearity $(B|C+D) = (B|C) + (B|D)$ and conjugate symmetry $(B|C)^* = (C|B)$ are quite obvious. But positivity $(B|B) \geq 0$ is less so. Using closure relations in terms of the eigenbasis of \mathbf{H} we can write the scalar product as follows:

$$(B|B) = \frac{1}{\beta} \int_0^\beta d\lambda g(\lambda) \sum_{nm} e^{(\lambda-\beta)E_n - \lambda E_m} |\langle m|B|n \rangle|^2. \quad (46)$$

In this form, we see that all the terms in the summation are positive. Since $g(\lambda)$ is also positive, the integrand is positive everywhere on the integration domain. Consequently, the formula is positive.

Finally, the Liouvillian is hermitian with respect to this scalar product:

$$\begin{aligned} (B|\mathcal{L}C) &= \frac{1}{\beta} \int_0^\beta d\lambda g(\lambda) \langle e^{\lambda \mathbf{H}} \mathbf{B}^\dagger e^{-\lambda \mathbf{H}} [\mathbf{H}, \mathbf{C}] \rangle \\ &= \frac{1}{\beta \text{Tr}[e^{-\beta \mathbf{H}}]} \int_0^\beta d\lambda g(\lambda) \text{Tr} [e^{(\lambda-\beta) \mathbf{H}} \mathbf{B}^\dagger e^{-\lambda \mathbf{H}} \mathbf{H} \mathbf{C} - e^{(\lambda-\beta) \mathbf{H}} \mathbf{B}^\dagger e^{-\lambda \mathbf{H}} \mathbf{C} \mathbf{H}] \\ &= \frac{1}{\beta \text{Tr}[e^{-\beta \mathbf{H}}]} \int_0^\beta d\lambda g(\lambda) \text{Tr} [e^{(\lambda-\beta) \mathbf{H}} \mathbf{B}^\dagger \mathbf{H} e^{-\lambda \mathbf{H}} \mathbf{C} - e^{(\lambda-\beta) \mathbf{H}} \mathbf{H} \mathbf{B}^\dagger e^{-\lambda \mathbf{H}} \mathbf{C}] \\ &= \frac{1}{\beta} \int_0^\beta d\lambda g(\lambda) \langle e^{\lambda \mathbf{H}} [\mathbf{B}^\dagger, \mathbf{H}] e^{-\lambda \mathbf{H}} \mathbf{C} \rangle \\ &= \frac{1}{\beta} \int_0^\beta d\lambda g(\lambda) \langle e^{\lambda \mathbf{H}} [\mathbf{H}, \mathbf{B}]^\dagger e^{-\lambda \mathbf{H}} \mathbf{C} \rangle \\ &= (\mathcal{L}B|C) \end{aligned} \quad (47)$$

Fermionic Green's function

The practical definition of the many-body retarded Green function and spectral weight for fermions in a system at equilibrium are

$$G_{rr'}^+(t) = -i \langle \{ \mathbf{c}_r(t), \mathbf{c}_{r'}^\dagger(0) \} \rangle \theta(t) \quad (48)$$

$$A_{rr'}^+(t) = \langle \{ \mathbf{c}_r(t), \mathbf{c}_{r'}^\dagger(0) \} \rangle \quad (49)$$

where $\mathbf{c}_r^{(\dagger)}(t)$ is the annihilation (creation) operator for a fermion at position r (and possibly other degrees of freedom) at time t and the fermion operators obey the canonical anticommutation relation: $\{c_r, c_{r'}^\dagger\} = \delta_{rr'} \mathbf{I}$ and $\{c_r, c_{r'}\} = 0$.

This leads us to choose the following scalar product:

$$(B|C) = \langle \{ \mathbf{C}, \mathbf{B}^\dagger \} \rangle. \quad (50)$$

This scalar product corresponds to eq. (44) with $g(\lambda) = \beta(\delta(\lambda) + \delta(\beta - \lambda))$. Thus, it satisfies all the necessary properties.

Bosonic Green's function

The usual definition of the retarded Green function and spectral weight when dealing with bosons are

$$G_{rr'}^-(t) = -i \langle [\mathbf{b}_r(t), \mathbf{b}_{r'}^\dagger(0)] \rangle \theta(t) \quad (51)$$

$$A_{rr'}^-(t) = \langle [\mathbf{b}_r(t), \mathbf{b}_{r'}^\dagger(0)] \rangle \quad (52)$$

where $\mathbf{b}_r^{(\dagger)}(t)$ is the annihilation (creation) operator for a boson at position r (and possibly other degrees of freedom)

at time t and the boson operators obey the canonical commutation relation: $[b_r, b_{r'}^\dagger] = \delta_{rr'} \mathbf{I}$ and $[b_r, b_{r'}] = 0$.

This hints at $(B|C) = \langle [\mathbf{C}, \mathbf{B}^\dagger] \rangle$ for scalar product. This scalar product is eq. (44) with $g(\lambda) = \beta(\delta(\lambda) - \delta(\beta - \lambda))$. This violates the positivity condition. Therefore, this isn't a valid inner product for the recursive method. The choice of a commutator instead of an anticommutator is a matter of convenience, and in this case, it is rather inconvenient. So we advise using the anticommutator scalar product for bosonic Green's function as well. Indeed, it is straightforward to obtain the commutator spectral weight eq. (52) from the anticommutator spectral weight eq. (49) using the detailed balance relation between two terms present in both of the functions. We define $A_{rr'}^>(t) = \langle \mathbf{b}_r(t) \mathbf{b}_{r'}^\dagger \rangle$ and $A_{rr'}^<(t) = \langle \mathbf{b}_{r'}^\dagger \mathbf{b}_r(t) \rangle$. Using the trace cyclic property, we can show that

$$A_{rr'}^>(t - i\beta) = A_{rr'}^<(t) \quad (53)$$

$$\implies e^{-\beta\omega} A_{rr'}^>(\omega) = A_{rr'}^<(\omega). \quad (54)$$

Since $A^+(\omega) = A^>(\omega) + A^<(\omega)$ and $A^-(\omega) = A^>(\omega) - A^<(\omega)$, it follows from eq. (54) that

$$A_{rr'}^-(\omega) = \tanh\left(\frac{\beta\omega}{2}\right) A_{rr'}^+(\omega). \quad (55)$$

The corresponding Green function can be obtained using eq. (29), if needed. Alternatively, one can compute each of the two terms of the commutator separately, by assigning to each of them their own inner product, similarly to what is done in the following section.

Zero temperature Hamiltonian limit

A special case of the Liouvillian formalism as presented here is the recursive method at zero temperature in the Hamiltonian formalism. The Hamiltonian formalism has one very significant advantage: it only involves operator acting on states. The algebra of operators acting on state is a significantly smaller burden than that of operators and superoperators, using it when possible can lead to significantly faster numerical computations.

In the Hamiltonian formalism, the recursion method must be applied once per term in the spectral weight [1, 6]. To replicate this feature in the Liouvillian formalism, we must define two inner products, one for each of the two terms in the Green's function:

$$(B|C)^+ = \langle \mathbf{C} \mathbf{B}^\dagger \rangle \quad (56)$$

$$(B|C)^- = \langle \mathbf{B}^\dagger \mathbf{C} \rangle. \quad (57)$$

Those scalar products correspond to eq. (44) with $g^+(\lambda) = \beta\delta(\lambda)$ and $g^-(\lambda) = \beta\delta(\beta - \lambda)$, respectively. The fermionic Green function is then $G_{rr'}(t) = [(c_{r'}|c_r(t))^+ + (c_{r'}|c_r(t))^-] \theta(t)$. The manipulations to be done are similar for both terms. Taking the zero tempera-

ture limit, the Lanczos coefficient are

$$\alpha_k^- = \langle \Omega | \mathbf{f}_{k,-}^\dagger (\mathbf{H} - E_0) \mathbf{f}_{k,-} | \Omega \rangle \quad (58)$$

$$\beta_k^- = \langle \Omega | \mathbf{f}_{k,-}^\dagger (\mathbf{H} - E_0) \mathbf{f}_{k-1,-} | \Omega \rangle \quad (59)$$

$$\alpha_k^+ = \langle \Omega | \mathbf{f}_{k,+} (\mathbf{H} - E_0) \mathbf{f}_{k,+}^\dagger | \Omega \rangle \quad (60)$$

$$\beta_k^+ = \langle \Omega | \mathbf{f}_{k-1,+} (\mathbf{H} - E_0) \mathbf{f}_{k,+}^\dagger | \Omega \rangle \quad (61)$$

where $|\Omega\rangle$ is the non-degenerate ground state and $\mathbf{f}_{0,\pm} = \mathbf{c}_r$. We observe that we can express both the Lanczos' coefficient eqs. (9,10) and the recursion relation eq. (8) in terms of the states $|\psi_k^\pm\rangle = \mathbf{f}_{k,\pm} | \Omega \rangle$. Indeed, by multiplying the recursion relation by the ground state we obtain

$$\beta_{k+1}^- |\psi_{k+1}^- \rangle = (-(H - E_0) - \alpha_k^-) |\psi_k^- \rangle - \beta_k^- |\psi_{k-1}^- \rangle \quad (62)$$

and

$$\beta_{k+1}^+ |\psi_{k+1}^+ \rangle = (H - E_0 - \alpha_k^+) |\psi_k^+ \rangle - \beta_k^+ |\psi_{k-1}^+ \rangle. \quad (63)$$

These two recursion relations on states are exactly what one finds when applying Lanczos method to the computation of Green's function within the Hamiltonian formalism [pyqcm,these,Dagotto].

III. MODEL

To illustrate the recursion method, we will apply it to the study the fermionic Hubbard model on a 2×2 plaquette. Finite realizations of the Hubbard model such as this are relevant to cluster methods [6, 24–27]. This family of methods yields an approximate Green's function of a lattice model from the Green's function computed from related cluster models such as the Hubbard plaquette we consider here. With methods of that nature, only lattice quantities expressible in terms of the Green's function can be computed for the lattice.

The Hubbard Hamiltonian is

$$H = t \sum_{\langle r,r' \rangle \sigma} (\mathbf{c}_{r'\sigma}^\dagger \mathbf{c}_{r\sigma} + \mathbf{c}_{r\sigma}^\dagger \mathbf{c}_{r'\sigma}) + U \sum_r \mathbf{c}_{r\uparrow}^\dagger \mathbf{c}_{r\downarrow}^\dagger \mathbf{c}_{r\downarrow} \mathbf{c}_{r\uparrow} - \mu \sum_{r\sigma} \mathbf{c}_{r\sigma}^\dagger \mathbf{c}_{r\sigma} \quad (64)$$

where r is a position on the plaquette, $\sigma \in \{\uparrow, \downarrow\}$ is the spin index, t is the hop amplitude, U the on-site Hubbard interaction and μ the chemical potential. $t \equiv 1$ defines the energy scale. We will consider the intermediate coupling regime $U = 4$ and at half-filling $\mu = \frac{U}{2}$. In this particular realization, all four sites are equivalent, and the model is spin symmetric. Due to the model finiteness, no phase transition can happen and no symmetry can be broken spontaneously. Thus, we make use of all available symmetry: it is enough to compute the Green's function elements at $r = (0, 0)$ and $r' \in [(0, 0), (0, 1), (1, 1)]$ and only for one spin population to reconstruct the Green's function in its entirety.

The complete Hilbert space for this model has size $4^4 = 256$. Consequently, commonly available linear algebra implementations are good enough to compute results in very

little time for this particular model. Here we use numpy to perform the numerical computations. For this problem, we perform full diagonalization of the plaquette Hamiltonian \mathbf{H} and compute the density matrix $\rho = \frac{\exp(-\beta\mathbf{H})}{\text{Tr}(\exp(-\beta\mathbf{H}))}$. The scalar product eq. (50) is used to compute the retarded Green's function eq. (48). Much more care and efforts would be needed to tackle larger finite models with this category of methods. Indeed, the cost of manipulating operators in a given Hilbert space is comparable to that of manipulating a state in a system twice the size and full diagonalization of the problem Hamiltonian is not practical for only slightly larger problems.

We perform a temperature dependence study of the plaquette by computing its local density of states and heat capacity using Green's function using exclusively continued fractions. This demonstrates the capability of this method to accurately compute various equilibrium quantities, as the system's free energy can be reliably determined if the heat capacity can be accurately computed. Additionally, we compare the off-diagonal element of Green's function obtained by LCCF (Eqs. (16,17)) with the CFPH procedure eq. (40). This comparison shows that the CFPH procedure reproduce the same spectral weight as the LCCF to high accuracy, with significantly fewer computations.

Results

In Fig. 1, we can see the evolution of the local density of states with temperature. The local density of states as shown in the figure is

$$D(\omega) = A_{00}(\omega) = \frac{-1}{\pi} \text{Im}(G(w + 0.2i)). \quad (65)$$

The limit to real frequency is not taken, leading to a lorentzian broadening of the Dirac deltas that would otherwise be present at real frequencies. We observe that most of the temperature driven changes occur before $T = 1$ and that by $T \approx 2.5$ the infinite temperature limit is almost reached. At $T \approx 0.3$ a significant amount of spectral weight is visible in the Mott gap. This is a hint of the metal-insulator transition in the lattice limit. As temperature rises, this weight within the gap keeps getting larger, a clear sign that the metallic phase is favoured by higher temperature.

As temperature rise from 0, the number of peaks visible in the spectrum increase significantly. At zero temperature, the exact density of state has sixteen poles, many of which have weights so small that they are not visible. Consequently, the Lanczos algorithm naturally stops after 16 iterations. As temperature rises the number of poles in the exact solution rise quickly and before $T = 0.055$ it becomes limited to 40, the maximum number of iterations of the Lanczos algorithm we allowed for those computations. From then on, the total number of poles present in the solution is fixed and their position lose their exact correspondence to excited states eigenvalues. At $T = 0.055$, most of the temperature driven changes to the spectrum has yet to

happen: the changes we observe happen through a reorganization of the available poles.

In practice, the limited development needs not limit the accuracy of computations, thermodynamic quantities show a good convergence rate with the maximum number of poles allowed. Figures 2 and 3 illustrate this quite neatly. In those we compute the constant volume heat capacity as a function of temperature using the Green's function and compare the resulting estimate with the numerically exact value. The exact value is obtained by computing

$$C_v(T) = \frac{1}{T^2} (\langle \mathbf{H}^2 \rangle - \langle \mathbf{H} \rangle^2) \quad (66)$$

using the density matrix. The Green function estimate is obtained by numerical derivation with respect to inverse temperature of the total energy:

$$E(T) = \frac{1}{2} \text{Tr} \left[\oint_C dz (z + H_0) F_T(z) G_T(z) \right] \quad (67)$$

$$C_v(T) = \left(\frac{\delta E(T)}{\delta T} \right)_v = \frac{-1}{T^2} \left(\frac{\delta E(T)}{\delta \beta} \right)_v \quad (68)$$

where $F_T(z)$ is the Fermi-Dirac distribution at temperature T , H_0 is the one-body Hamiltonian matrix and the closed integration path C contains all the poles of the Green's function $G_T(z)$ and none of the poles of Fermi-Dirac's distribution. The numerical derivative is done with the symmetric finite difference formula

$$\frac{\delta E(\beta)}{\delta \beta} = \frac{E(\beta + \Delta) - E(\beta - \Delta)}{2\Delta} + O(\Delta^2), \quad (69)$$

with an inverse temperature variation $\Delta = 0.01$.

In Fig. 2, we observe a good qualitative agreement with the exact result with as few as 10 floors to the continued fractions used. Indeed, all the expected feature are present in roughly the right position, with similar relative amplitudes. With only 20 floors in the continued fractions, the agreement is nearly quantitative; the absolute error is less than 0.1, as can be seen in Fig. 3. With 40 and 60 floors to the continued fractions, quantitative agreement is reached for all values. Note that at temperature above 1, the heat capacity computations gradually become independent of the number of poles; the computations' accuracy is limited by the finite difference formula which has error $O(10^{-4})$. Since this approach to computing heat capacity depends on an accurate computation of the total energy, it means that the free energy can also be computed accurately. Indeed, the free energy is [12]

$$\begin{aligned} F(T) &= E(T) - TS(T) = E(T) - T \int_0^T dT_0 \frac{C_v(T_0)}{T_0} \\ &= E(0) - T \int_0^T dT_0 \frac{E(T_0) - E(0)}{T_0^2}. \end{aligned} \quad (70)$$

Consequently, any quantity that can be expressed as a derivative of the free energy can be computed with an error comparable to that of the heat capacity.

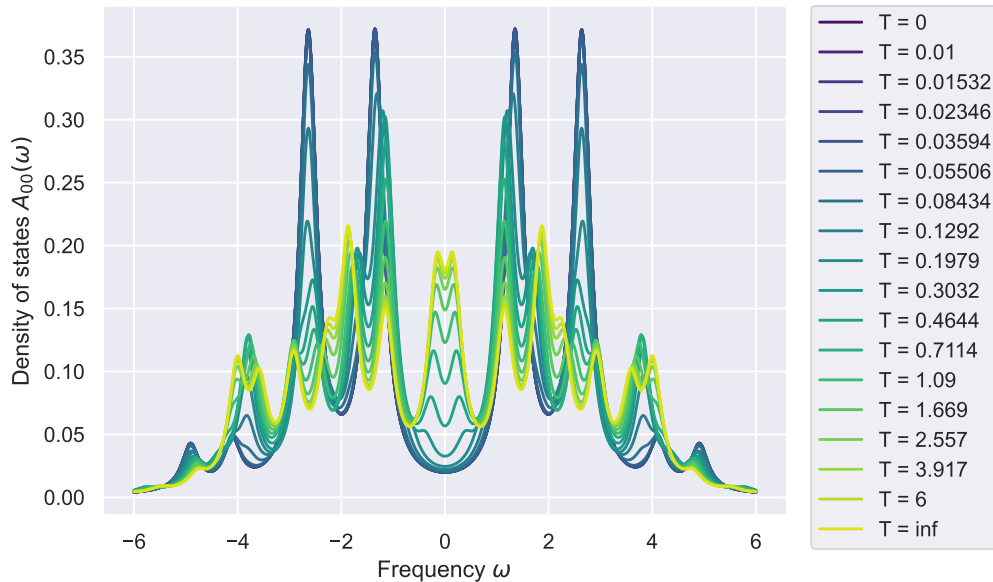


Figure 1. Local density of state as a function of frequency at temperatures ranging from 0 to infinity with lorentzian broadening $\eta = 0.2$ and at half-filling with $U = 4$. The density of states is computed by taking the imaginary part of the local Green's function at a given temperature. The Green's function is represented in the form of a continued fraction with $k = 40$ maximum floors. At low temperatures, fewer than 40 floors are needed.

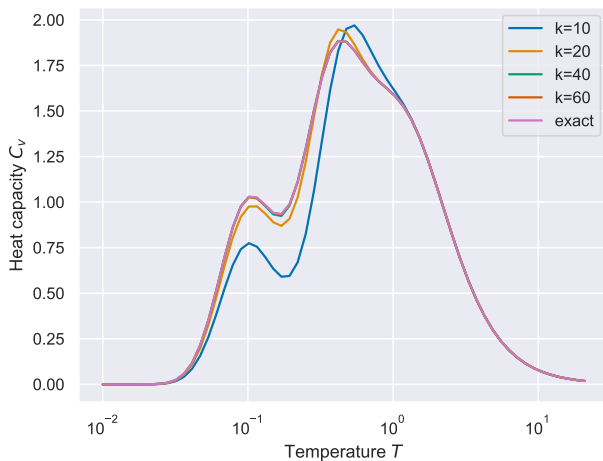


Figure 2. Heat capacity of the 2x2 Hubbard plaquette as a function of temperature at half-filling with interaction $U = 4$. The different k values are the maximum number of floors to the continued fractions, the exact result is computed directly from the density matrix.

In Fig. 4 we show the spectral weight of the three irreducible contribution to the entire spectral weight, computed with the Lanczos-Polynomial hybrid method. The result of the linear combination of continued fraction approach to the computation of off-diagonal elements are not shown because there would be no visible difference. Indeed, the resulting spectral weights are numerically equivalent to what is obtained from, as is shown in Fig. 5. We observe there that the most pronounced difference is less

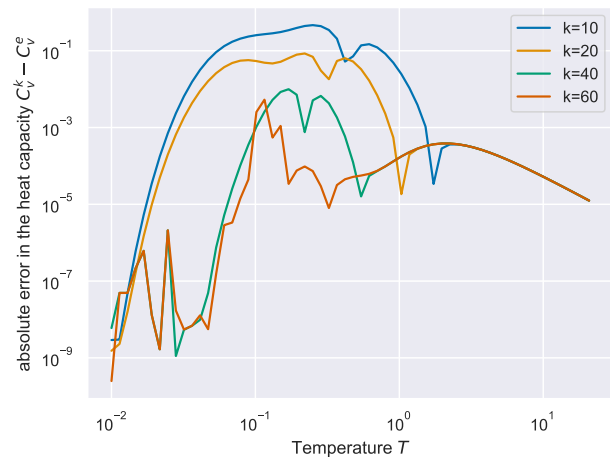


Figure 3. Error in the heat capacity with respect to the numerically exact computation.

than 10^{-10} .

Computing all three irreducible elements of the Green's function of this particular model can be done in a single recursive procedure, needing only one extra inner product computation per iteration per off-diagonal elements, bringing the total number of operations to k application of the Liouvillian and $(2+o)k$ inner product computations, where $k \leq 40$ is the number of iterations of the recursion process and $o = 2$ is the number of off-diagonal Green function elements to compute. This is in contrast to $(o+1)k$ application of the Liouvillian and $2ok$ inner products of the LCCF method.

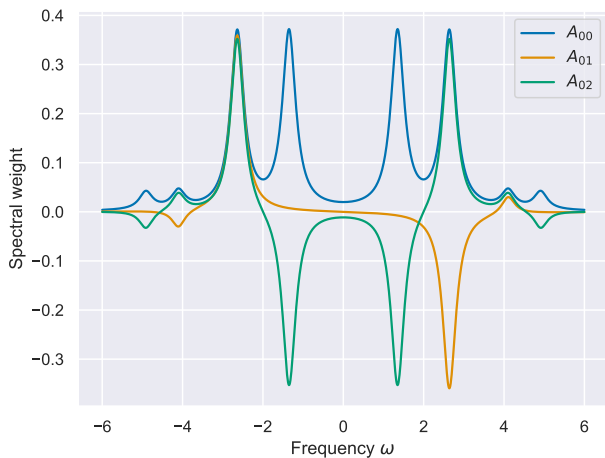


Figure 4. Spectral weight, on-site (A_{00}), at first neighbours (A_{01}) and second neighbours (A_{02}) at inverse temperature $\beta = 80$ with lorentzian broadening $\eta = 0.2$.

IV. CONCLUSION

In conclusion, we have presented a comprehensive and simplified framework for the recursion method. This framework allows for the computation of response functions for a wide range of quantum operators within the Liouvillian formalism, including non-Hermitian operators. Notably, we have shown that the Hamiltonian formalism of the recursion method is a special case of the Liouvillian recursion method.

While we have focused on a toy problem, it is important to note that the recursion method has already been successfully applied to problems of interest in condensed matter. Its ability to accurately compute response functions and extract valuable information from quantum many-body systems has been demonstrated in previous studies. The gen-

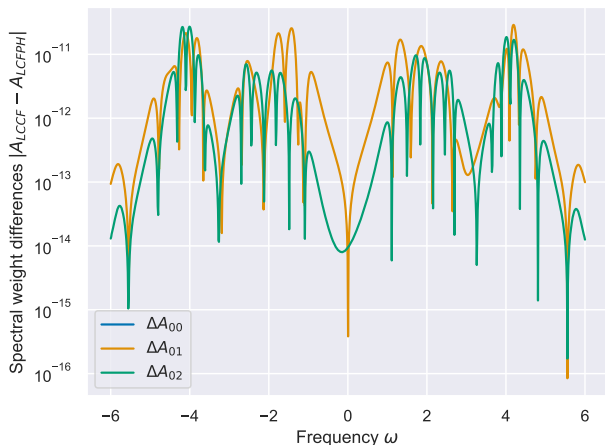


Figure 5. Absolute difference in the spectral weights computed with the Lanczos-polynomial hybrid method and the linear combination of continued fractions method.

erality and flexibility of the method make it a good tool for investigating a wide range of strongly correlated systems.

However, further efforts are required to design and implement efficient algorithms and techniques specifically tailored to larger and more realistic systems. Tensor network methods, for instance, show promise in addressing the computational challenges associated with larger systems. With tensor networks, time and memory needs are nominally polynomials. These methods offer polynomial time and memory requirements, but the accuracy depends on the choice of a parameter, the bond dimension. The precise effect of that parameter on accuracy is problem dependent and its contribution to computational complexity depends on network topology. Consequently, constant precision complexity is often discovered through empirical means. For limited order development, we find an alternative in variational representations of the thermodynamic state along with a sparse representation of the operator generated by the recursive relations. In addition to the complexity of producing the equilibrium state, the worst-case time and memory needs are of order $O(N^k)$ where N is the number of terms in the sparse representation of the Hamiltonian and k is the order to which the recursive procedure is carried out. Variational solutions on near-term quantum computers holds particular interest as a potential application for the recursion method.

In summary, the recursion method provides a powerful and versatile approach for computing response functions in quantum many-body systems. By further refining its algorithms and combining it with complementary techniques, we are confident that complex quantum materials can be better understood.

ACKNOWLEDGMENTS

Thanks to professors Maxime Charlebois, André-Marie Tremblay and David Sénéchal for insightful discussions and encouragement. Thanks to my colleagues Jean-Frédéric Laprade, Maxime Dion, Marco Armenta, Tania Belabas, Ghislain Lefebvre and Christian Sara-Bournet for their help, support and encouragement. This work has been supported by the Canada First Research Excellence Fund and the Ministère de l'économie, de l'innovation et de l'énergie du Québec.

-
- [1] V. S. Viswanath and G. Müller, *The recursion method: application to many-body dynamics*, Lecture notes in physics No. m23 (Springer-Verlag, Berlin ; New York, 1994).
- [2] H. Mori, A Continued-Fraction Representation of the Time-Correlation Functions, *Progress of Theoretical Physics* **34**, 399 (1965).
- [3] M. H. Lee, Orthogonalization Process by Recurrence Relations, *Physical Review Letters* **49**, 1072 (1982).
- [4] M. H. Lee, Derivation of the generalized Langevin equation by a method of recurrence relations, *Journal of Mathematical Physics* **24**, 2512 (1983).
- [5] U. Balucani, M. Howard Lee, and V. Tognetti, Dynamical correlations, *Physics Reports* **373**, 409 (2003).
- [6] T. N. Dionne, A. Foley, M. Rousseau, and D. Sénéchal, Pyqcm: An open-source Python library for quantum cluster methods, *SciPost Physics Codebases* , 023 (2023).
- [7] E. Dagotto, Correlated electrons in high-temperature superconductors, *Reviews of Modern Physics* **66**, 763 (1994).
- [8] A. Georges, G. Kotliar, W. Krauth, and M. J. Rozenberg, Dynamical mean-field theory of strongly correlated fermion systems and the limit of infinite dimensions, *Reviews of Modern Physics* **68**, 13 (1996).
- [9] Xavier Barnabe-Theriat, *ANALYSE A TAILLE FINIE DU POIDS SPECTRAL DU MODELE DE HUBBARD* (2003).
- [10] A. Prémont-Foley, *Réseaux de tenseurs et solutionneurs d'impureté pour la théorie du champ moyen dynamique*, Ph.D. thesis, Université de Sherbrooke (2020).
- [11] N. Hatano and M. Suzuki, Finding Exponential Product Formulas of Higher Orders, *arXiv:math-ph/0506007* **679**, 37 (2005).
- [12] See supplemental materials [url] (2023).
- [13] A. Weisse, G. Wellein, A. Alvermann, and H. Fehske, The Kernel Polynomial Method, *Reviews of Modern Physics* **78**, 275 (2006).
- [14] F. A. Wolf, I. P. McCulloch, O. Parcollet, and U. Schollwöck, Chebyshev matrix product state impurity solver for dynamical mean-field theory, *Physical Review B* **90**, 10.1103/PhysRevB.90.115124 (2014).
- [15] J. C. Wheeler, Modified moments and continued fraction coefficients for the diatomic linear chain, *The Journal of Chemical Physics* **80**, 472 (1984).
- [16] M. Ganahl, M. Aichhorn, H. G. Evertz, P. Thunström, K. Held, and F. Verstraete, Efficient DMFT impurity solver using real-time dynamics with matrix product states, *Physical Review B* **92**, 155132 (2015).
- [17] M. Dressel and G. Grüner, *Electrodynamics of solids: optical properties of electrons in matter* (Cambridge University Press, Cambridge ; New York, 2002).
- [18] A. Cuyt, W. B. Jones, V. B. Petersen, B. Verdonk, and H. Waadeland, *Handbook of Continued Fractions for Special Functions* (Springer Science+Business Media B.V., Dordrecht, 2008).
- [19] A. I. Zayed, ed., *Handbook of Function and Generalized Function Transformations*, 1st ed. (CRC Press, 2019).
- [20] H. S. Wall, *Analytic theory of continued fractions* (2018) oCLC: 1039341362.
- [21] R. Groux, Sur une mesure rendant orthogonaux les polynômes secondaires, *Comptes Rendus Mathématique* **345**, 373 (2007).
- [22] J. Sherman, On the numerators of the convergents of the Stieltjes continued fractions, *Transactions of the American Mathematical Society* **35**, 64 (1933).
- [23] P. K. Jain, O. P. Ahuja, and K. Ahmad, *Functional analysis*, 2nd ed. (New Age International, New Delhi, 2004).
- [24] M. Guillot, *Compétition entre l'antiferromagnétisme et la supraconductivité dans le modèle et Hubbard appliqué aux cuprates*, Master's thesis, Université de Sherbrooke (2007).
- [25] K. Seki, T. Shirakawa, and S. Yunoki, Variational cluster approach to thermodynamic properties of interacting fermions at finite temperatures: A case study of the two-dimensional single-band Hubbard model at half filling, *Physical Review B* **98**, 205114 (2018).
- [26] M. Aichhorn, E. Arrigoni, M. Potthoff, and W. Hanke, Variational cluster approach to the Hubbard model: Phase-separation tendency and finite-size effects, *Physical Review B* **74**, 235117 (2006).
- [27] P. Sahebsara and D. Sénéchal, Hubbard Model on the Triangular Lattice: Spiral Order and Spin Liquid, *Physical Review Letters* **100**, 136402 (2008).